SSRG International Journal of Mechanical Engineering
ISSN: 2348-8360/ https://doi.org/10.14445/23488360/IJME-V12I8P102

Volume 12 Issue 8, 12-19, August 2025

Original Article

Design and Analysis of a Cross-Plane Solenoid Engine for Torque Ripple Stability in Electric Vehicles

Lee Eunjune[1], Kim Eunseo[2], Kim Sunjae[3], Kim Gyeonmin[4]

[1,2,3,4]*Department of Mechanical Engineering, Gaon, Gyeonggi-do, Republic of Korea.*

[1]*Corresponding Author : eunjune1208@gmail.com*

Received: 03 June 2025 Revised: 04 July 2025 Accepted: 05 August 2025 Published: 29 August 2025

Abstract - *The Internal Combustion (IC) engine is recognized as one of the major contributors to environmental pollution. Consequently, the demand for alternative fuels has been increasing due to the depletion of fossil fuel reserves and increasing environmental concerns. However, electric motors can cause instability at lower speeds, caused by torque ripples, which cannot be effectively resolved via the original motor structure. To tackle this problem, this paper proposes utilizing the boxer engine structure with a cross-plane crankshaft. To leverage this structural advantage of the IC engine, this study designs a solenoid-based engine, integrating the boxer engine composition and cross-plane crankshaft design. Since significant motion is not observed in the prototype engine. The present study, therefore, conducts a diagnosis of the engine's failure to operate as intended, then gives a detailed analysis of the underlying causes and proposes potential solutions. Through numerical analysis, this study evaluates the efficiency of the refined engine.*

Keywords - *Electric engines, Electromagnetic forces, Electromagnetic inductions, Engine stabilities, Motors.*

1. Introduction

A significant time has passed since the initial attempts to make use of fossil fuels successfully provided mankind with an abundant energy supply. However, as excessive use of fossil fuels began causing pollution and global environmental harm, efforts to decrease reliance on the fuels increased. This shift is well represented in the development of electric cars [1, 2].

The utilization of electric motors is noticeable in emerging vehicles, which is distinguishable from the Internal Combustion (IC) engines that traditional cars widely adopted. Though these new systems were environment-friendly and could contribute to the reduction of fossil fuel consumption, they still had mechanical issues to resolve.

A slow-driving vehicle suffers from vibration and instability specifically attributed to the structural limits of the electric motors. This is due to the lack of inherent damping and mass distribution characteristics of the IC engines. This instability can negatively affect driving performance, especially under urban conditions where there are a lot of stop-and-go conditions.

Therefore, the primary objective is to develop and set a basis for solenoid-based engines. This seeks to combine the structural benefits of IC engines with the environmental benefits of electric engines. Solenoid-based engines have been studied in several papers [3–7].

The former studies on solenoid engines focused simply on crafting the engine. Further, changing the cylinder into a solenoid in the largely studied V-type or L-type engines was their sole purpose. They neglected the reason why such studies are needed and why they are valuable. For instance, "An Electromagnetic Mechanism Which Works Like an Engine" by Shirsendu Das shows a lack of explanation of a study while providing the methods to make a solenoid-infused inline engine. "Design and Fabrication of 4-Stroke Solenoid Engine" by Anamika et al. also failed to mention the work's significance, and it constructs a boxer engine without explaining the reasons for using the specific structure [3, 4].

In contrast to earlier research, this paper constructs its work with a certain objective: To reduce vibration and ripple. Unlike former efforts, methods to infuse and utilize a boxer engine and a cross-plane engine in new structures were at the bottom of this project. This discussion presents the advantages of solenoid-based engine designs and establishes the necessity of similar and continued research in this field based on these insights. In this paper, a combination of a boxer engine and a cross-plane crankshaft was designed to reduce the vibration at lower speeds.

2. Theoretical Background

The vibration of an engine is largely classified into primary and secondary vibrations, which is a fundamental

concept that must be understood beforehand to comprehend the structural characteristics of the engine.

For pistons that are not in the power stroke and do not contribute to the crankshaft rotation at that moment, their circular motion is converted into linear reciprocating motion inside the cylinder as the crankshaft rotates. The reciprocating motion of the piston causes its primary vibration. Because the piston undergoes a complete up-and-down cycle for every full rotation of the crankshaft, this vibration occurs at the same frequency as the engine's rotational speed. This type of vibration is inherent in all reciprocating engines, but its effects can be minimized through careful counterweight placement on the crankshaft or the use of additional balancing mechanisms.

Secondary vibration, in contrast, results from the non-uniform acceleration of the piston due to the mechanical and geometrical constraints of the crankshaft and connecting rod. Unlike primary vibration, this oscillation occurs at twice the crankshaft's frequency, meaning the piston experiences two oscillations per revolution.

This effect is particularly noticeable at high RPMs, where secondary vibration can cause additional mechanical fatigue, structural stress, and unwanted noise. While smaller in magnitude compared to the primary vibration, this secondary component plays a crucial role in engine dynamics, as it can contribute to mechanical stress, increased noise, and even resonance issues if left unaddressed.

Depending on the arrangement of pistons and the relative position of the crankshafts, engines are categorized into different structures. An understanding of the various structures is crucial to ultimately selecting one that fits to minimize motor vibration. The structure and explanations of the boxer engine are as follows.

Boxer engines are a sort of flat engine. The angle between each crankpin measures 180˚, allowing a symmetrical motion about the middle of the engine. The corresponding 180˚ gap of the two cylinder banks enables a reduced height compared to other engines. A boxer engine's superiority is shown in its low height and proportioned piston motion. Its low height lowers the center of mass, increasing the driving stability. The mirror-imaged motion of the pistons promotes neutralizing secondary vibration, as demonstrated in the following section.

$$x = r\cos\theta + l\cos\Phi \tag{1}$$

Here, x stands for the position of the piston. And r, θ denotes the distance between the main journal and the crankpin, and the rotated angle of the crank, respectively. l and Φ are for the length of the connecting rod and the angle of it.

Using the Fourier series to convert the Equation (1) into the Equation (2), the periodic function of the second term can be converted into a sum of trigonometric functions.

$$x = r\cos\theta + \frac{r^2}{4l}\cos\theta \tag{2}$$

The first term represents the basic motion of the piston. Because the piston's displacement follows a cosine function, this term directly corresponds to the crankshaft's rotational frequency. In other words, the piston completes one full stroke per crankshaft revolution, making this term the dominant component of its movement. The second term accounts for secondary vibration, which arises due to the geometric constraints of the connecting rod. Since the connecting rod has a finite length, the piston does not move at a perfectly uniform rate throughout its stroke. This introduces a second-order oscillation, which occurs at twice the crankshaft's rotational frequency.

One of the key advantages of a Boxer engine is its partial offset of secondary vibrations due to its unique piston arrangement. In a Boxer engine, pistons are positioned in horizontally opposed pairs, meaning that as one piston moves upward, its counterpart moves downward with an identical motion but in the opposite direction. Because these opposing pistons generate secondary oscillatory forces of equal magnitude but opposite directions, the net effect is the mutual cancellation of secondary vibrations. As a result, a Boxer engine operates with significantly reduced secondary vibration compared to L-type or V-type engines, which often require balance shafts or additional countermeasures to mitigate vibration.

In the case of primary vibrations, they can be canceled out because of their symmetrical motion. However, its structural traits make it easy to err in manufacturing the actual engine, demoting its ability to moderate the vibration.

The crankshaft is one of the important parts of this paper. Crankshafts have two structural types, and the decision between the two options is crucial to attain the paper's objective. In this paper, the cross-plane crankshaft, which is more effective in reducing torque ripple, is used.

Cross-plane crankshafts are structures in which the cranks hold the same crankpin gap of 90˚ with another crank group. It is known to apply a more regular force compared to the other crankshaft structures. This design brings about an alteration in acceleration due to changes in crankshaft angles, suppressing secondary vibrations. As opposed to flat-plane crankshafts, there is no need for extra components to counteract vibration, showing its great performance in vibration cancellation. The downside is that it is heavier and more expensive than the other crankshafts. The unique structure and the required exhaust pipe design contribute to its high cost.

3. Numerical Calculation

The inductance of the coil is produced from the equation below.

$$L = \mu_0 \cdot N^2 \cdot \frac{A}{d} \quad (3)$$

The permeability of free space, μ_0 has a value of $4\pi \cdot 10^{-7} H/m$. N is for the number of turns of the coil, A for the cross-sectional area, which is the inertial area of the solenoid through which the magnetic field passes. And d stands for the length of the coil wrapped around the solenoid. The value of each variable used in this paper is, respectively, 460 turns, $1{,}225mm^2$, $62mm$. The calculated inductance is detailed below.

$$L = \mu_0 \cdot 460^2 \cdot \frac{1{,}225}{62} = 5.26mH \quad (4)$$

The calculated resistance and current are detailed below.

$$R = \rho_{Cu} \cdot \frac{l}{A} = 0.222\Omega \quad (5)$$

$$I_{applied} = \frac{V_{applied}}{R} = 216.22A \quad (6)$$

Where R denotes the resistance of the coil, ρ_{Cu} is the resistivity of copper, l is the length of the wire comprising the coil, $I_{applied}$ is the applied current, and $V_{applied}$ denotes the applied voltage.

The magnetic field strength inside a solenoid is proportional to the number of turns of the coil and applied current, while having an inverse proportionality to the length of the coil.

$$B = \mu_0 \cdot \frac{N \cdot I_{applied}}{l} = 2.016T \quad (7)$$

The magnetic moment of a permanent magnet is calculated using the equation below.

$$m = M \cdot V \quad (8)$$

Here, the volume of the magnet and the magnetization are each represented as V and M. Magnetization is the quantity that determines how strongly a material becomes magnetized when exposed to an external magnetic field, and is a product of B_{mag}(magnetic field due to a material's magnetization, or magnetic flux density) over μ_0. The magnet used in this study, a neodymium magnet, has a value of 1.3T in magnetic flux density.

$$M = \frac{B_{mag}}{\mu_0} = 1.035 \times 10^6 A/m \quad (9)$$

V equals $6.08 \times 10^{-7} m^3$, the magnetic moment of the magnet is as shown below.

$$m = 0.6293A \cdot m^2 \quad (10)$$

Suppose the strength of the field decreases to 0 on both ends of the solenoid. This allows us to approximate the gradient of B, the rate of change in the magnetic field over distance, by B over half the length of the coil.

$$\nabla B \approx \frac{B}{0.5 \cdot l} = 65.03T/m \quad (11)$$

Consequently, the value of the exerted force on the magnet is a product of ∇B and the magnetic moment.

$$F = m \cdot \nabla B = 40.92N \quad (12)$$

Torque, a rotational form of force, is produced by the expansion of Equation (12), which is needed to later process rotating systems.

$$\tau = F \cdot r \cdot \sin\theta \quad (13)$$

In Equation (13), r stands for the distance between the center of the main journal and the crankpin, in this research, 35mm. θ is the rotated angle of the crankshaft. For a convenient calculation process, we presume the sine value to always be 1 for any different θ values.

$$\tau = 40.92N \times 0.035m \times 1 = 1.432N \cdot m \quad (14)$$

The RPM of a crankshaft is calculated using the piston's average speed. In the equation below, its speed is expressed as V_p.

$$RPM = \frac{V_p}{2r} \times 60 \quad (15)$$

The traveled distance of 31mm over a time of 1ms estimates to an RPM value of $26{,}570RPM$.

$$RPM = \frac{31 \times 10^{-3}}{1 \times 10^{-3}} \times \frac{60}{2 \times 35 \times 10^{-3}} = 26{,}570RPM \quad (16)$$

The engine's horsepower results from an equation of torque and RPM.

$$P[W] = \frac{2\pi}{60} \times \tau \times RPM = 3{,}984.5W \quad (17)$$

$$P[HP] = \frac{P[W]}{745.7} = 5.345HP \quad (18)$$

4. Materials and Methods

4.1. Engine Structure Design

In this study, the position of the coils was established considering the mutual inductance between each solenoid coil. The length of the crankshaft was then determined to fit this spacing. In the following passages, the process to obtain mutual inductance will be described.

$$M = k\sqrt{L_1 L_2} \quad (19)$$

Above, k is a symbol for the coupling coefficient, and L_1, L_2 for the inductance of two different coils. The mutual inductance calculation utilises Equations (5) and (20).

$$M = k\sqrt{L_1 L_2} = k \cdot 5.26mH \tag{20}$$

The coupling coefficient k has a maximum value of 1 when two coils are extremely close to each other, gradually decreasing as they gap further. k expressed as a function of its distance is inscribed below.

$$k(d) = k_0 \times e^{-a \cdot d} \tag{21}$$

k_0 and a are each the coupling coefficient at zero distance and the magnetic field attenuation constant. Ideally, k_0 approximates to 1, and a varies between $0.1 \sim 0.5 m^{-1}$ within the air medium. In Figure.1, we have drawn the results of Equation (22) as a function of the gap distance, having adjusted the value of two constants as such: $k_0 = 0.5, a = 0.1$.

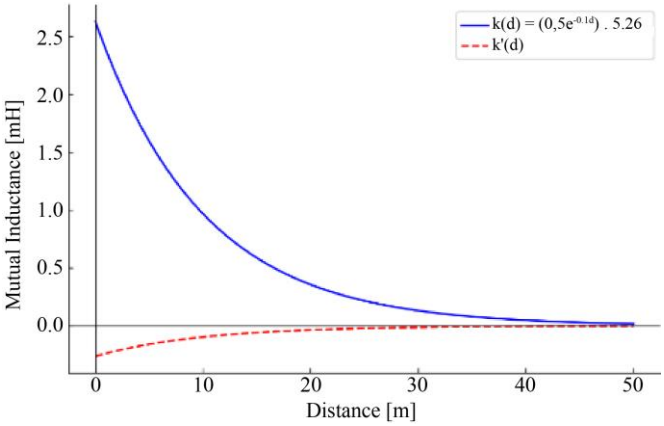

Fig. 1 Function of mutual inductance and its derivative

For the optimization of the engine size, the longer distance between two coils was set to 1 meter. Based on these settings, the 3D modeling of the engine generated can be seen in Figure.2. The magnetic field when voltage is induced in a single coil is visualized below in Figure 3.

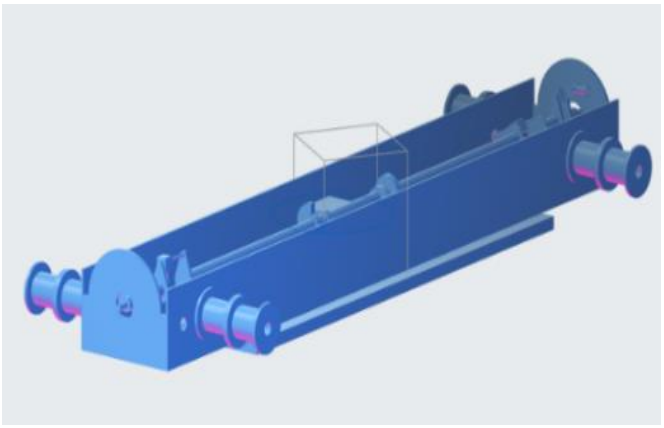

Fig. 2 3D view of the engine

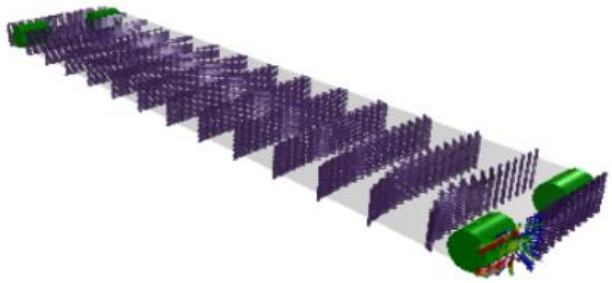

Fig. 3 Visualization of magnetic fields

By evenly positioning the four rotary switch actuators in a 90˚ gap, we have enabled the voltage to the coils according to the crankshaft's angle. For stable transport at slow speeds, the cross-plane crankshaft was selected, which ensures stable operation due to having more segments of angles than a flat-plane crankshaft. Also, the design was formed in a boxer engine structure in the hope of minimizing the vibration that comes from the typical IC engine structure.

4.2. Circuit Design

In this paper, the engine was designed to have four switch-coil pairs, each switch corresponding to one coil. The design was originally intended for a relay-switched induct circuit where the coil is induced with voltage changes as the crankshaft presses different switches while spinning. The circuit diagram is illustrated below.

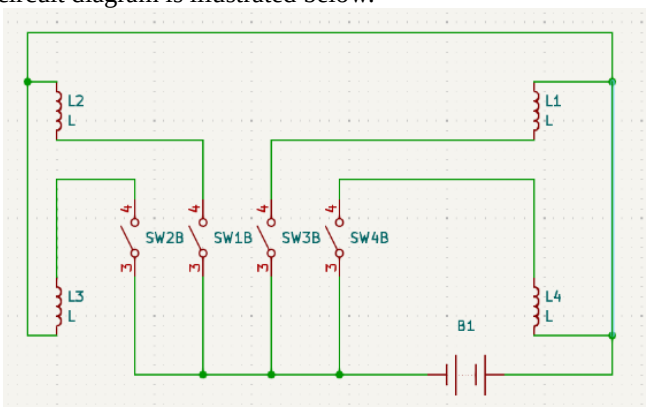

Fig. 4 Relay switch inductor circuit

4.3. Fabrication of the Engine

The parts comprising the crankshaft are fabricated from a commonly used aluminum alloy, Al6061. The components are shown in Figure 5.

The assembled crankshaft of the paper has a stroke of 74.4mm and a bore of 10mm, which makes it an undersquare engine specializing in low rpm motors. The engine frame is depicted in Figure 6.

The completed model, which includes the crankshaft, is shown below as Figure 7.

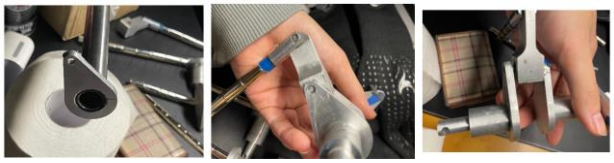

(a) (b) (c)

Fig. 5 Crankshaft parts. (a) crank throw, and (b)&(c) piston & connecting rod & crank throw.

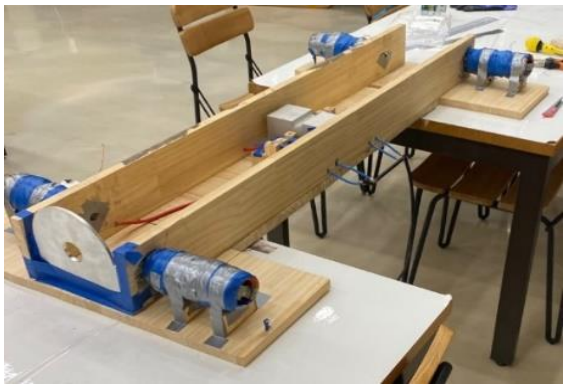

Fig. 6 Engine frame

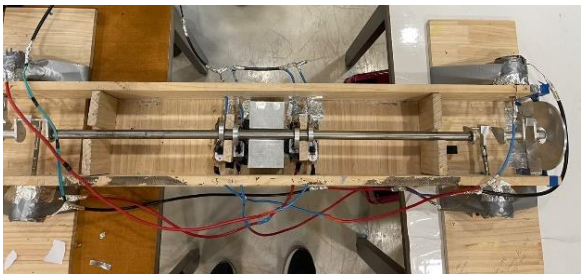

Fig. 7 Engine assembled

4.4. Analyzis and Redesigning of the Study

4.4.1. Analyzis of the Study – the Reason for Its Failure

The solenoid engine crafted for the study did not function as intended. The following text analyzes the reason for its failure.

Bias of Force on the Crankshaft

The engine utilized a cross-plane crankshaft, four-cylinder structure, where a single piston was connected to four crank throws, each displaying different angles. On the two ends of the crankshaft, about as long as 1.4 meters, are located two crank throws with a 90˚ gap in between. Due to its feature where a maximum voltage of only two coils is applied over the same period, force is applied on only one end of the crankshaft. The long crankshaft makes an uneven balance, creating yaw and causing it to revolve around the middle holding block of the engine. A certain amount of force, originally intended to spin the crankshaft, is used for a different direction, exerting lower levels of torque than expected.

With the decrease in torque, the movement of the crankshaft due to yaw makes a change in the angle at which force is applied. A shift in angle occurs in connecting rods and pistons, which must be aligned with the cylinder, resulting in an impediment to their movement. Not only does it disturb the application of forces in the intended direction, but it also has the potential to cause various problems. The separation of magnets that make up the piston and the jamming of this piston itself in the cylinder are a few examples.

Error in the Structural Design

The other problem we expected to be the reason for failure is the insufficient formation of clearance for the parts to spin. The long crankshaft makes an uneven balance, creating yaw and causing it to revolve around the middle holding block of the engine. As a result of this, we believe it is okay to blame an action of strong friction due to the lack of distinct clearance.

By design, the length of the crankpin was just about identical to the width of the connecting rod. The friction area of the joint where the crankpin and connecting rod, the connecting rod and piston meet does not have enough room to allow for unproblematic movement. Also, providing a space too tight for lubricants defeats the idea of somewhat moderate friction. This is why we infer that a strong friction must have taken place in the rotating process.

4.4.2. Adjusting Design Errors

We redesigned the four-cylinder boxer engine structure into an eight-cylinder one. Making the two crank throws face each other with a 180˚ gap between. This structure was devised to prevent the yaw of the crankshaft. It enabled a symmetrical application of force by dividing the rotating angle into four 90˚ units and connecting two pistons to each unit. The design accounting for all the feedback is depicted in Figures 8 and 9, showing the new crank throw structure joined with the crankshaft.

This design symmetrically applies force from the two ends of the crankshaft, preventing too much force from being applied to one side.

The long crankshaft makes an uneven balance, creating yaw and causing it to revolve around the middle holding block of the engine. Therefore, when no electric force is induced, the junction spot of the piston and connecting rod is located along the center of the main journal. When electricity is induced, the connecting rod rotates about the crankpin due to the piston's force, rather than receiving the force while staying perpendicular to the ground surface. This not only produces the rotating motion of the crankshaft, but it also causes roll in the piston itself. The center axis of the piston and the direction of the magnetic force do not align, causing the magnets and coils to form a magnetic field weaker than what was designed.

This error can be overcome by tuning the connecting rods, pistons, and solenoids. By adjusting the inner diameter of the solenoid coil to the stroke, we design the moving piston so that

it does not get stuck with the connecting rod. Also, by matching the piston's bore with the coil's diameter, the roll of the piston can be prevented. This way, we make the center axis of the piston always be aligned with the solenoid's center axis. Finally, we match the connecting rod's length with the stroke so that the piston can have the minimum length without slipping out of the cylinder pocket.

As mentioned above, by rearranging the clearance between the connecting points of each part, a space to supply lubricant can be obtained. This results in a decrease in friction, which occurs as rotational action continues.

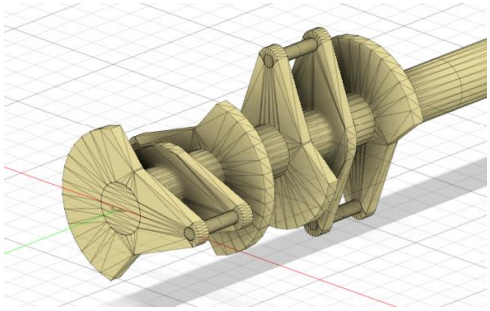

Fig. 8 Configuration of the adjusted crank throw

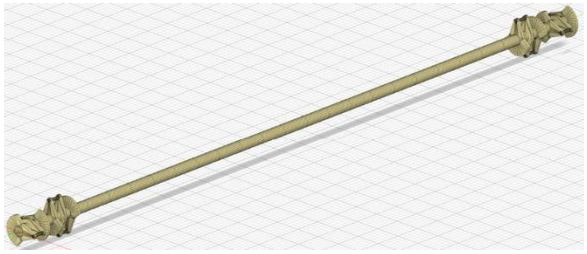

Fig. 9 8-cylindered crankshaft with the adjusted crank throw

4.4.3. Numerical Analyzis of the Refined Study

Referring to Equation (13), the value of torque concerning angle θ is such.

$$\tau = 40.92 \times 0.035 \times sin(\theta) \tag{22}$$

In a cross-plane crankshaft, there is a change in force every 90˚ rotation. The equation that reflects this phenomenon can be expressed as a function of time [8].

$$\tau = 1.4322 \times sin\left(\frac{\pi}{2} - \left(100\pi t \ mod \frac{\pi}{2}\right)\right) \tag{23}$$

$$\tau = 1.4322 \times cos\left(100\pi t \ mod \frac{\pi}{2}\right) \tag{24}$$

Let the torque be calculated above. τ_{piston}, then the net torque is the total accumulation of τ_{piston} with friction torque, τ_f.

$$\tau_{net} = \tau_{piston} + \tau_f \tag{25}$$

In Equation (25), τ_f. represents the viscous friction torque, which can be expressed as the product of the viscous friction coefficient, radius, and angular velocity. Considering the direction of torque, the viscous friction torque is given as follows.

$$\tau_f = -cr\omega \tag{26}$$

Here, c denotes the viscous friction coefficient, which typically ranges between 0.2 and 0.05 for metals lubricated with oil. In this study, a value of 0.1 is assumed. r represents the radius of the crank to which friction is applied, which is 10mm. ω is the angular velocity can be derived through the following process.

$$I\frac{d\omega}{dt} = \tau_{net} = \tau_{piston} + \tau_f \tag{27}$$

The moment of inertia I of the crankshaft is defined in terms of the mass m of the crank and its radius r.

$$I = \frac{1}{2}mr^2 \tag{28}$$

Rearranging Equation (27) using Equation (24) and Equation (26) returns the following equation.

$$I\frac{d\omega}{dt} = 1.4322\ cos\left(100\pi t \ mod \frac{\pi}{2}\right) - cr\omega \tag{29}$$

$$\frac{d\omega}{dt} + \frac{cr}{I}\omega = \frac{1.4322\ cos\left(100\pi t \ mod \frac{\pi}{2}\right)}{I} \tag{30}$$

This equation is a first-order linear differential equation, which can be solved using the following method. The general form of a first-order linear differential equation is given as such.

$$\frac{dy}{dt} + P(x)y = Q(x) \tag{31}$$

By applying the integrating factor method, the general solution is acquired as follows.

$$y = e^{-P(x)} \int e^{P(x)} Q(x) dx \tag{32}$$

Employing this in Equation (30), with an initial condition of $\omega = 0$ at $t = 0$, results in the following equation.

$$\omega = e^{-\frac{cr}{I}t}\left[\frac{1.4322}{I}\int e^{\frac{cr}{I}t}\ cos\left(100\pi t \ mod \frac{\pi}{2}\right) dt\right] \tag{33}$$

Thus, τ_f is given as follows.

$$\tau_f = -cre^{-\frac{cr}{I}t}\left[\frac{1.4322}{I}\int e^{\frac{cr}{I}t}\ cos\left(100\pi t \ mod \frac{\pi}{2}\right) dt\right] \tag{34}$$

In Equation (33), the limiting speed of the angular velocity can be confirmed by how the value appears when 't' diverges to infinity. In order to confirm this mathematically, the equation in which the term of the transient response is removed from Equation (33) is as follows.

$$\omega = \frac{1.4322}{I} \int e^{\frac{cr}{I}t} cos\left(100\pi t \; mod \frac{\pi}{2}\right) dt \quad (35)$$

Given that the crank weighs 4.27kg and has a radius of 10mm, the moment of inertia of the crankshaft can be determined using Equation (28) as follows.

$$I = \frac{1}{2} \times 4.27 \times 0.01^2 = 0.0002135 \quad (36)$$

Therefore, the angular velocity can be summarized as follows.

$$\omega = 6707.57 \times \int e^{4.684t} cos\left(100\pi t \; mod \frac{\pi}{2}\right) dt \quad (37)$$

5. Results and Discussion

The angular velocity is presented graphically in Figure 10. The point where the rate of angular velocity, excluding ripple effects, drops below 0.1rad/s² is approximately 11.99s. Beyond this point, the angular velocity can be considered as the limiting angular velocity.

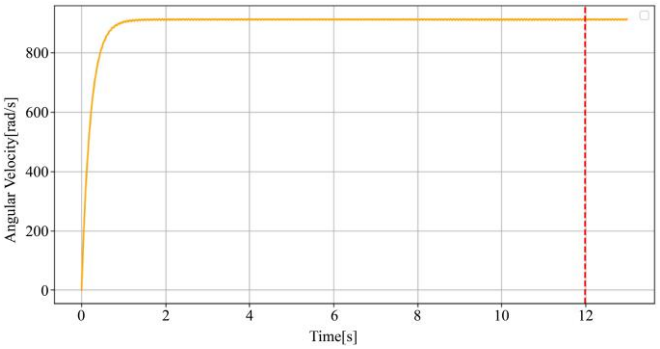

Fig. 10 $\omega - t$ graph.

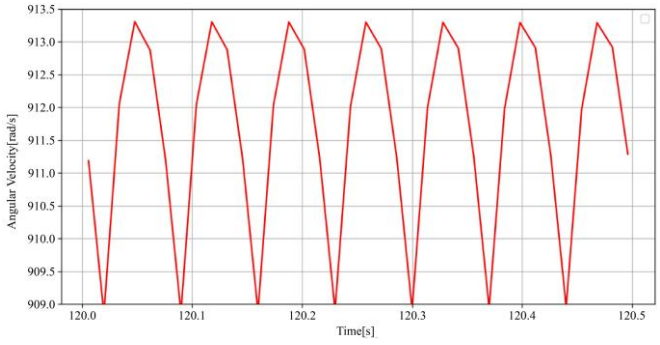

Fig. 11 ripple shown in $\omega - t$ graph.

Magnifying the angular velocity within the limited angular velocity range produces a graph of Figure. 11.

In the given graph, the ripple period is approximately 0.07s, corresponding to a frequency of approximately 14.3Hz. Additionally, the angular velocity in the stable boundary is approximately 911.2rad/s, and the ripple amplitude is approximately 2rad/s. Converting this amplitude into RPM is shown in the following value.

$$RPM_{stable\ boundary} = \frac{911.2}{2\pi} \times 60 \approx 8700RPM \quad (38)$$

$$RPM_{maximum\ ripple} = \frac{911.2+2}{2\pi} \times 60 \approx 8713.7RPM \quad (39)$$

$$RPM_{minimum\ ripple} = \frac{911.2-2}{2\pi} \times 60 \approx 8686.3RPM \quad (40)$$

The RPM fluctuation is ±13.7 RPM, which falls well below the generally perceivable range of 50–100 RPM at high rotational speeds exceeding 8,000 RPM.

6. Conclusion

Based on the above calculations, in Results and Discussion, the engine's torque ripple corresponds to approximately 50–100 RPM, which translates to a frequency range of about 0.83–1.67 Hz. Although this falls within the range of frequencies perceptible to the human body, it is generally difficult to detect in practice. Therefore, the vibrations generated during the operation of the cross-plane-applied eight-cylinder solenoid boxer engine are expected to be hard for the human body to notice. Additionally, given the shortened force application cycle, it is expected that torque ripple can be reduced compared to electric motors that operate similarly to conventional flat-plane crankshafts. This serves as theoretical evidence suggesting that the application of this engine structure can positively contribute to torque ripple reduction and enhanced driving stability.

Conflicts of Interest

The authors declare that there are no competing interests regarding the authorship and publication of this paper. This study was conducted purely for academic purposes, without any financial benefit obtained from individuals, institutions, corporations, or other stakeholders throughout the research process. Furthermore, the study was not carried out with the intention of pursuing commercial interests, patent acquisition, or product development, and there is no possibility that the results have been influenced by any external economic or political factors. The authors affirm that the entire research process was conducted independently and autonomously to ensure objectivity and integrity.

Funding Statement

This research was supported financially by Gaon High School for expenses necessary during the research and experimental process.

Acknowledgments

I would like to express my profound appreciation to all those who allowed us to successfully conclude this study. I am grateful to our project supervisor, Mr.Yoo, whose efforts extend to giving guidance and feedback throughout our research. I also want to extend my thanks to Gaon High School for their financial support, as their assistance has been invaluable.

References

[1] Simone Franzò, and Alessio Nasca, "The Environmental Impact of Electric Vehicles: A Novel Life Cycle-Based Evaluation Framework and its Applications to Multi-Country Scenarios," *Journal of Cleaner Production*, vol. 315, 2021. [CrossRef] [Google Scholar] [Publisher Link]

[2] Jihyeok Jung et al., "Factors Affecting Consumers' Preferences for Electric Vehicle: A Korean Case," *Research in Transportation Business & Management*, vol. 41, 2021. [CrossRef] [Google Scholar] [Publisher Link]

[3] Anamika Tiwari et al., "Design and Fabrication of 4-Stroke Solenoid Engine," *International Research Journal of Engineering and Technology*, vol. 6, no. 12, pp. 2819-2825, 2019. [Google Scholar] [Publisher Link]

[4] Shirsendu Das, "An Electromagnetic Mechanism Which Works Like an Engine," *International Journal of Engineering Trends and Technology*, vol. 4, no. 6, pp. 2376-2379, 2013. [Google Scholar] [Publisher Link]

[5] Ejazmallik Ansari et al., "Design and Fabrication of Single Cylinder Solenoid Engine," *Anveshana's International Journal of Research in Engineering and Applied Sciences*, vol. 7, no. 2, pp. 1-11, 2022. [Google Scholar] [Publisher Link]

[6] Piyush Hota, Mahima Rathore, and Danish Shaikh, "Magnetic Repulsion Piston Engine," *International Journal of Science and Research*, vol. 4, no. 12, pp. 338-344, 2015. [Google Scholar] [Publisher Link]

[7] Navdeep Singh et al., "RPM Variable Solenoid Engine," *Mediterranean Journal of Basic and Applied Sciences*, vol. 5, no. 4, pp. 1-12, 2021. [CrossRef] [Google Scholar] [Publisher Link]

[8] Yannik Louvigny, and Pierre Duysinx, "Advanced Engine Dynamics Using MBS: Application to Twin-Cylinder Boxer Engines," *IMSD 2010 (The 1st Joint International Conference on Multibody System Dynamics)*, Lappeenranta, Finland, pp. 1-10, 2010. [Google Scholar] [Publisher Link]